RASĀYAN *J. Chem.*
Vol. 15 | No. 1 |509-515| January - March | 2022
ISSN: 0974-1496 | e-ISSN: 0976-0083 | CODEN: RJCABP
http://www.rasayanjournal.com
http://www.rasayanjournal.co.in

MULTIFUNCTIONAL $Cr_xCa_{(10-x)}Al_{30}Si_{60}$ GLASSES, ELECTRICAL CONDUCTIVITY AND THERMOLUMINESCENCE

Kodumuri Veerabhadra Rao[1,2,✉], Padala Ashok[1] and B. Appa Rao[1]
[1]Department of Physics, University College of Science, Osmania University, Hyderabad-500 007, Telangana, India
[2]Department of Physics, Humanaties and Science, Methodist College of Engineering and Technology, Osmania University, Abids-500 001, Telangana, India
✉Corresponding Author: veerabadhraraokodumuri@gmail.com

ABSTRACT

The SiO_2 glasses embedded with Cr^{3+} ions are notable for solid state optical resource, which are useful in various opto-electronic and semiconducting applications. However, the available thermoluminescent resource, which include different electronic and semiconducting materials, need some refinement in their structure, luminescence, and electronic properties towards development of advanced glass resource. In this vision, $Cr_xCa_{(10-x)}Al_{30}Si_{60}$ glassy materials have planned for synthesis and testing. The GT, and GC phase transition points, and thermal stability (~1.2639) of test samples are identified. Structural vibrations are identified with the help of FT-IR spectra. The order of electrical conductivity ($\sim 1.657 \times 10^{-4}$ ohm^{-1} cm^{-1}), and A.E. (~0.3669 eV) of test samples reveal their electrical strength. The symmetry (~ 0.576%) factor, frequency (1.1172×10^{20} S^{-1}) factor, and A.E. (0.682 eV) of the test samples are recorded under 30 kGy irradiation. Overall, the results, which include structure, electrical and luminescence of the test samples suggest the materials might be useful electrically conductive and thermal stimulated light resource.

Keywords: CaO-Al_2O_3-SiO_2-Cr_2O_3Glasses, X-Ray Diffraction, DTA, FT-IR, Electrical Conductivity, Thermoluminescence.

RASĀYAN*J. Chem.*, Vol. 15, No.1, 2022

INTRODUCTION

Inherently, the glass with silicon dioxide chemical constitutes is highly non-corrosive, transparent, and thermally stable. Their anticipated properties, such as high refractive index and luminescence, will make them needful optoelectronic industrial applications.[1] Since many years to present, there have been wide-ranging research on a glasses with SiO_2 chemical constitutes due to their abnormal structure, and spectroscopic results.[2] The aluminum oxide is not a conventional glass former, but add-on Al_2O_3 to the glasses with SiO_2 improves their elastic nature, thermal stability, non-corrosion properties.[3-4] And also increase of Al_2O_3 in the SiO_2 glass host lead to more microhardness and thermal stability. SiO_2 embedded with Al_2O_3 glasses have a high order of thermally stimulated luminescence, which will highly useful for radiation dosimetry process.[5] The addition of CaO to the silicate glass substances enhance the refractive index, and optical inertness. Calcium silicate glasses embedded with different transition metal oxides are the most favorable candidates in the current semiconducting sectors and finds plentiful usage in the area of thermoluminescent and D.C. Conductivity applications.[6-7] The addition of Al_2O_3 also influence SiO_2 ions, which furtherimproves the strength, chemical endurance, mechanical and spectroscopic properties to a considerable extent of the overall glass network.[8] The CaO, and Al_2O_3 in the silicate glass host stimulates Cr^{3+} ions for better optical output. The metal oxide like Cr_2O_3 is a well-known nucleation agent, which involves tri-valent oxidation states in silica glass matrix to enhance thermoluminescence and D.C. conductivity properties.[9] Usually, Cr^{3+} ions have a substantial effect on the glass lattice, further which lead to advance in thermoluminescence and D.C. conductivity properties.[10] The glass with silicon dioxide chemical constitutes enclosing mixed valence states of Cr^{3+} ions are of recent interest as a thermoluminescence and cathode resource in rechargeable batteries as of their abnormal energy density,and capacitance.[11]

Subsequently, in the existing work, Cr_2O_3 doped calcium aluminum silicate materials were synthesized and report for their suitability regarding thermoluminescent and D.C. conductivity behavior.[12] Potential functions such as abnormal thermoluminescent and D.C. conductivity, etc., are achievable by improving tremendously advantageous solid-state glass resource that have fascinated extensive attention. Because of this, the current research aimed to prepare solid-state glass materials of chemical composition $Cr_xCa_{(10-x)}Al_{30}Si_{60}$and to study the (x)$Cr_2O_3$+(10-x)CaO composite influence on electricalconductivity, and TL characteristics of Al_2O_3+SiO_2 glasses.

EXPERIMENTAL

The chemicals of $Cr_xCa_{(10-x)}Al_{30}Si_{60}$ have taken for preparation of samples (where, $0.0 \leq x \leq 1.0$, step size = 0.2 mol %). The 99 % Pure AR grade chemicals such as Cr_2O_3, CaO, Al_2O_3, and SiO_2 have chosen in agate mortar for fine grinding. Finely grinded power, in required mol% is taken in crucible with a 25 ml volume for form a glass. The furnace operated upto 1470ºC temperature. Obtained melt allowed for rapid cooling on brass cast to achieve a test glass. Immediately, the achieved test glass annealed at 490ºC with help of other furnace. Refined, and dimensionally prepared test samples are taken for structure, electrical, and luminescence studies. The melt quenching technique is used to develop the test samples. The composition of test glasses given as follows **Cr-0.0** ($Cr_{0.0}Ca_{10}Al_{30}Si_{60}$), **Cr-0.2** ($Cr_{0.2}Ca_{9.8}Al_{30}Si_{60}$), **Cr-0.4**($Cr_{0.4}Ca_{9.6}Al_{30}Si_{60}$), **Cr-0.6**($Cr_{0.6}Ca_{9.4}Al_{30}Si_{60}$), **Cr-0.8**($Cr_{0.8}Ca_{9.2}Al_{30}Si_{60}$), and **Cr-1.0** ($Cr_{1.0}Ca_{9.0}Al_{30}Si_{60}$).

RESULTS AND DISCUSSION

Figure-1 reports the X-ray diffraction recording of $Cr_xCa_{(10-x)}Al_{30}Si_{60}$ glasses. The analysis suggest glassy behavior of the all the test samples. Figure-2 reports chemical analysis of the glass with 0.8 mol% Cr_2O_3concentration. Results obtained signify Ca, Al, Si, O, and Cr with their atomic weight %. Figure-3 reports, DTA spectra of the $Cr_xCa_{(10-x)}Al_{30}Si_{60}$ glasses. The glass transition (T_g), and crystallization (T_c) temperature positions are identified from the spectra. And thermal stabilities of glasses are computed with the help of glass transition (T_g), and crystallization (T_c) temperature. The variation in values of thermal stability of glasses with ion concentration projected in the inset of the same figure. Observed results reveal a glass with 0.8 mol% Cr_2O_3concentration exhibiting the highest in the values of thermal stabilities of current glasses.

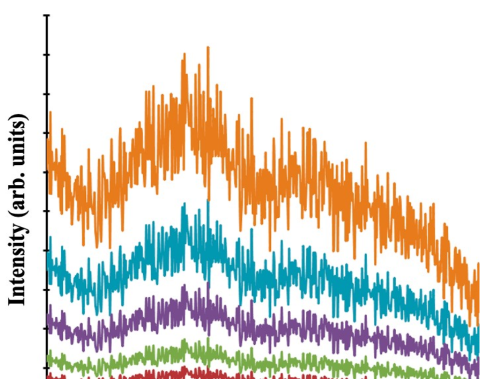

Fig.-1: X-Ray Diffraction Pattern of$Cr_xCa_{(10-x)}Al_{30}Si_{60}$GlassesConcentration

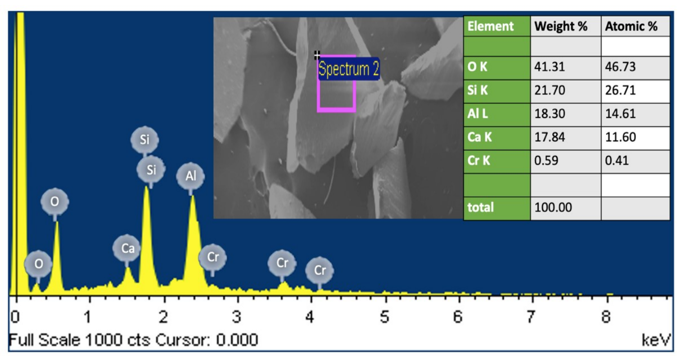

Fig.-2: Chemical Analysis of Glass with 0.8 mol% Cr_2O_3Concentration

All the exothermic and endothermic thermograms variations are observed highest for the glass with0.8 mol% Cr_2O_3concentration, due to enthalpy change.[13] Figure-4 reports the FT-IR spectra of $Cr_xCa_{(10-x)}Al_{30}Si_{60}$glasses. Observed spectra exhibited well resolved following bands due to silicate, lanthanum, and Cr^{3+}units at different wavenumber regions.[14-18] The Ca–O (~ 1575 cm^{-1}) linkages, AlO_4 (~ 415 cm^{-1}) linkages, AlO_6 (~ 710–775 cm^{-1}) linkages, Si–O–Si Asymmetrical (~1015 to 1023 cm^{-1}) stretching, Si–O–Si Symmetrical (~ 842 to 851 cm^{-1}) stretching, Si–O–Si Rocking /bending (~ 461 to 473 cm^{-1}) vibrations, Cr–O Specific (~ 415 cm^{-1}) stretching vibrations. The glass with a 0.8 mol% Cr_2O_3concentration found to be highest in the $Cr_xCa_{(10-x)}Al_{30}Si_{60}$ glasses exhibiting the highest shift in wavenumber positions of all the silicate, aluminum, calcium and chromium structural units. The FT-IR analysis supports all the existence various chemicals such as Si–O–Si asymmetrical, Si–O–Si symmetrical, Si–O–Si bending, AlO_6 distorted octahedral and Cr–O specific stretching vibrational units.

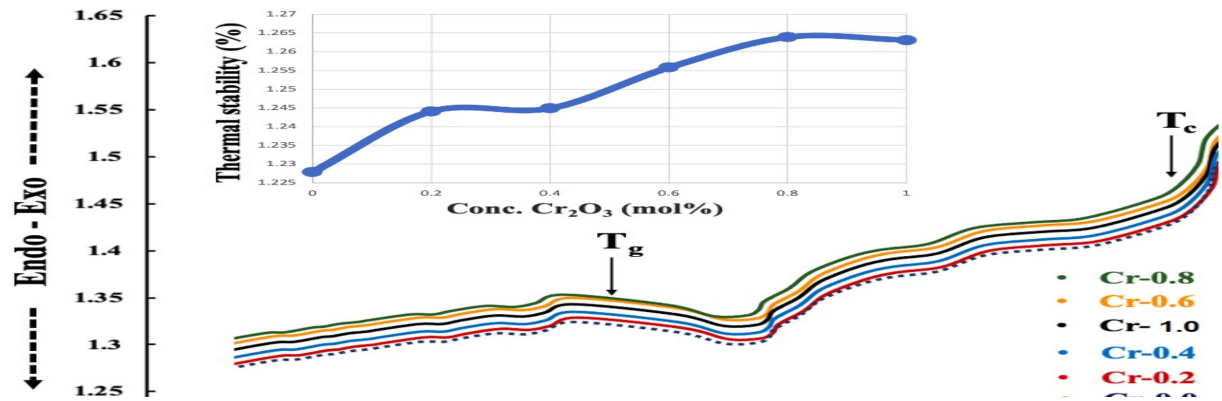

Fig.-3: DTA Thermograms of (10-x)CaO-30Al_2O_3-60SiO_2:xCr_2O_3Series of Glass Materials, (where, $0.0 \leq x \leq 1.0$, step size = 0.2 mol %). Inset (a) shows the variation in thermal stability with increasing concentration of Cr_2O_3

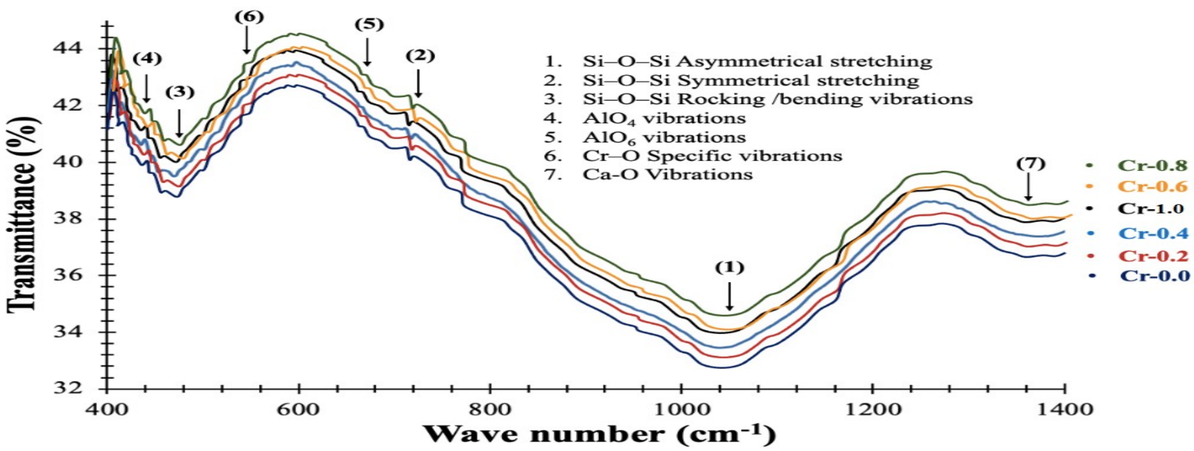

Fig.-4: FT-IR Spectra of $Cr_xCa_{(10-x)}Al_{30}Si_{60}$ Glass Materials recorded at Room Temperature with in the Wave Number Range of 400-1400 cm^{-1}

Glass with a 0.8 mol% Cr_2O_3 concentration found to be highest in the $Cr_xCa_{(10-x)}Al_{30}Si_{60}$ glasses exhibiting the highest shift in wavenumber positions of all the silicate, aluminum, calcium and Cr^{3+} structural units due to steady inter-ionic forces between Cr^{3+} ions to Si^{4+}, Al^{3+}, and Ca^{2+} ions.The tetrahedrons in SiO_2 geometry are observed to be interconnected with mutual corners sharing. Usually, SiO_2 in its amorphous form will be preferred for glass production. Usage of Al_2O_3 in SiO_2 glasses improves the hardness, refractive index, and density of optical glasses. It is also used to improve thermo and piezoelectric characteristics of SiO_2 glass. SiO_2 glass phosphors, conductive ceramics, and dielectrics inclusive of Al_2O_3 are valuable photoelectronic resources. Naturally, Al_2O_3 has Cr_2O_3 hexagonal symmetry at low temperatures. The addition of CaO and Cr_2O_3 actively involves with Ca^{2+} and Cr^{3+} ions produce Ca-O-Si and Cr-O-Si linkages, which further influence all other Si^{4+}, Al^{3+}, and Ca^{2+} ions within the glass network and improves non-bridging oxygen's.

Electrical Conductivity

Figure-6 illustrates electricalconductivity variations with the inverse of increasing temperature. Observed results are almost linear. Insect (a), and (b) of the figure signifies the variation in electricalconductivity and A.E. with Cr_2O_3 increasing concentration. Observed electricalconductivity increased up to 0.8 mol% Cr_2O_3 concentration. Whereas analyzed, A.E. found to be decreasing until 0.8 mol% Cr_2O_3 concentration increasing concentration.[19] All the evaluations concerning electrical conductivity measurements are observed to be highest for the Cr-0.8 glass code. The detailed information concerning electrical conductivity measurements of the $Cr_xCa_{(10-x)}Al_{30}Si_{60}$ glassesare furnished in Table-1.

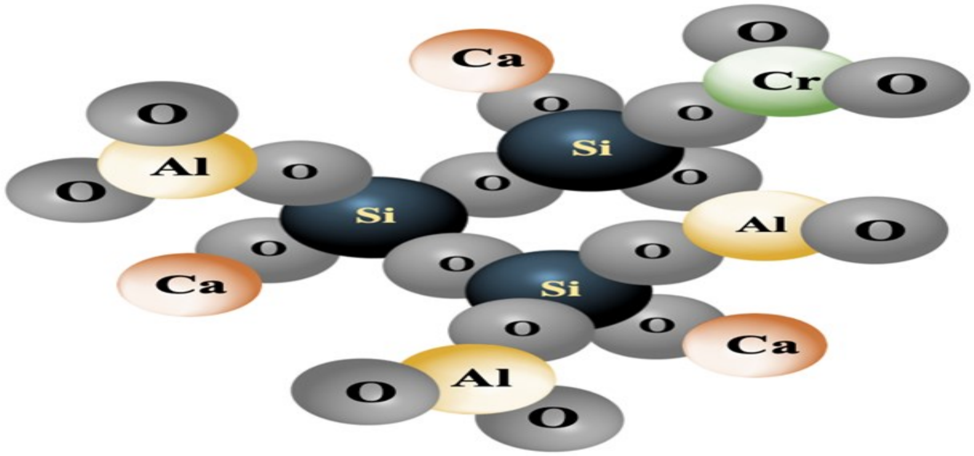

Fig.-5: Proposed Molecular Structure of $Cr_xCa_{(10-x)}Al_{30}Si_{60}$Glasses

Linear relation between electrical conductivity with increased inverse temperature in the present Cr - series of materials suggesting that the linear thermally exciting movement of the charge carriers for conduction An increase in the values of electrical conductivity and decrease in the values of A.E. up to 0.8 mol% Cr_2O_3 suggest a higher rate of polaron hopping and ionic transport phenomenon within the present Cr - series of materials. Mixed ionic and electronic conduction effects cause an increase in the value of electrical conductivity and a decrease in the values of A.E. up to 0.8 mol% Cr_2O_3 concentration.[20] In comparison, decreasing electrical conductivity and decrease in the values of A.E. after 0.8 mol% Cr_2O_3 concentration. Both analyses suggest dissimilar conduction phenomena on the two sides of the present chemical composition. Such variations in the values of both electrical conductivity and A.E. of the present Cr - series of materials due to conformed mobility of both Ca^{2+} and Cr^{3+} ions.

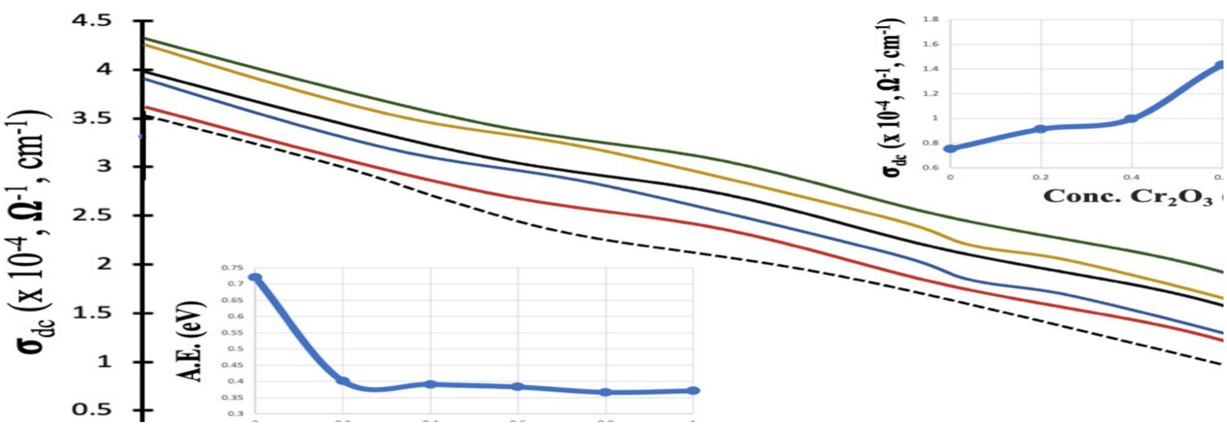

Fig.-6: Variation of Electrical Conductivity with 1/T for $Cr_xCa_{(10-x)}Al_{30}Si_{60}$ Glass Materials, (where, $0.0 \leq x \leq 1.0$, step size = 0.2 mol %). The inset 8(a) represents variation in activation energy with concentration and inset 8(b) variation in electrical conductivity with concentration of Cr_2O_3.

Table-1: Data on Electrical Conductivity of $Cr_xCa_{(10-x)}Al_{30}Si_{60}$ Series of glass materials, (where, $0.0 \leq x \leq 1.0$, step size = 0.2 mol %).

Glass	DC Conductivity at 300 K ($x\ 10^{-4}$ ohm^{-1} cm^{-1})	A.E. (eV)
Cr-0.0	0.755	0.7215
Cr-0.2	0.915	0.4015
Cr-0.4	0.997	0.3912

Cr-0.6	1.435	0.3833
Cr-0.8	1.657	0.3669
Cr-1.0	1.585	0.3715

Thermoluminiscence

Thermoluminescence of the $Cr_xCa_{(10-x)}Al_{30}Si_{60}$ glasses were recorded from room temperature to 300 ^{0}C without γ- irradiation, and under 30 minutes of γ- irradiation (~30 kGy), these reports are shown in Fig.-7. In both situations the luminescence intensity is increasing as increasing upto 0.8 mol% Cr_2O_3 concentration.

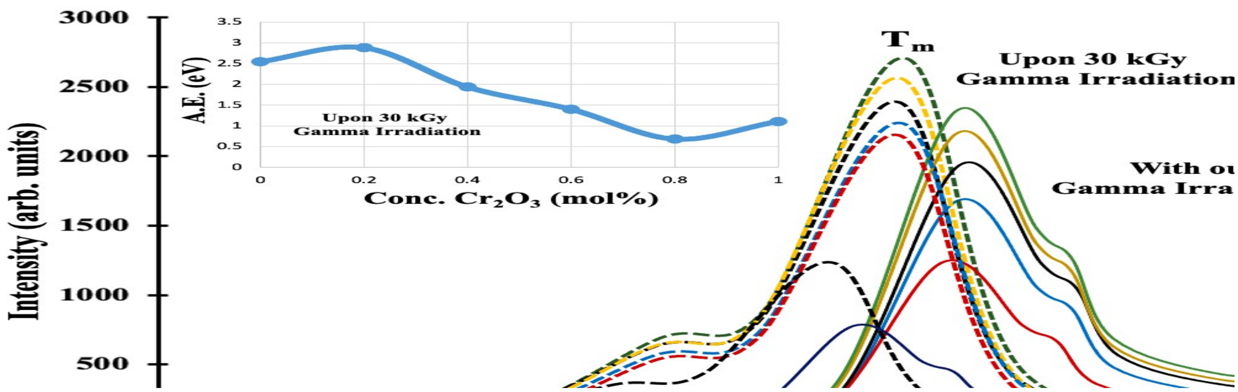

Fig.-7: Thermoluminiscence Analysis of $Cr_xCa_{(10-x)}Al_{30}Si_{60}$ Series of Glass Materials, (where, $0.0 \leq x \leq 1.0$, step size = 0.2 mol %).

The luminescence graph shows two intensity peaks for every glass sample one is at low temperature and other is at high temperature, the intensity peak at low temperature disappears quickly compare to intensity at high temperature. The trap-depth factors of glass samples were calculated by subsequent equations.[21-22]

$$E_x = C_x\left(\frac{KT_m^2}{x}\right) - b_x(2KT_m)$$

$$E_y = C_y\left(\frac{KT_m^2}{y}\right)$$

$$E_z = C_z\left(\frac{KT_m^2}{z}\right)$$

$$\text{Frequency Factor} = \frac{\beta E}{KT_m^2}\left(\frac{exp\left(\frac{E}{KT_m}\right)}{\left(1+(b-1)\frac{2KT_m}{E}\right)}\right)$$

Where, T_m is temperature at peak intensity,

T_1 = half maximum intensity intercepts at left and right side on the TL curve, and K is Boltzmann constant.

$x = T_m - T_1, y = T_2 - T_m, z = T_2 - T_1$ and Symmetry ratio$(\eta) = \frac{y}{z}$;

$C_x = 1.510 + 3(\eta - 0.42), C_y = 0.976 + 7.3\ (\eta - 0.42)$ and

$C_z = 2.52 + 10.2(\eta - 0.42), \quad b_x = 1.58 + 4.2(\eta - 0.42)$

The trap depth factors such as activation-energies (E_x, E_y, and E_z) and shape symmetry ratios without γ-irradiation and under 30 minutes of γ- irradiation witnessed from thermoluminescence investigation are initiate to be best for the glass sample of 0.8 mol% of Cr_2O_3 and the conforming data was provided in Table-2. The TL measurements of the $Cr_xCa_{(10-x)}Al_{30}Si_{60}$ glasses found to be increased, and the Cr-0.8 glass code found to be best in the results. Generally, Al_2O_3 exhibits (Al/Si)-O tri-clusters. Ca^{2+} ions and octahedral (Al/Si)-O_6 tri-clusters dislocate silicate linkages and induce binding defects. The addition of Al_2O_3 improves the structural defects within the glass network. Suitable applied external heat or thermal energy, lead to liberation of electrons, which also increase the Al^{3+}, Cr^{3+}, Si^{4+}, and Ca^{2+} ions with in the samples. The irradiation on surface of sample induce trap centers. Which will increase in increasing with irradiation dose. Later on the thermal moment with in the samples lead to electron trapping with trap centers with in the materials. In this view, the sample with 08 Cr_2O_3 mol% concentration observed to be highest in TL grades.

Table-2: Summary on Thermoluminiscence Studies of $Cr_xCa_{(10-x)}Al_{30}Si_{60}$ Glass Materials, (where, 0.0 ≤ x≤ 1.0, step size = 0.2 mol %).

Glass	T_m (K)	u	E_x (eV)	E_y (eV)	E_z (eV)	E_{avg} (eV)	Frequency Factor (s^{-1})
Cr-0.0	428	0.5	2.366	2.191	2.288	2.282	4.5288 X 10^{30}
Cr-0.2	463	0.473	2.974	2.785	2.899	2.886	1.0143 X 10^{32}
Cr-0.4	465	0.44	2.714	2.554	2.652	2.640	2.0836 X 10^{21}
Cr-0.6	466	0.392	1.973	1.928	1.969	1.957	2.7914 X 10^{15}
Cr-0.8	471	0.333	1.839	1.744	1.819	1.800	6.6342 X 10^{7}
Cr-1.0	467	0.375	3.028	2.834	2.951	2.938	1.7510 X 10^{12}
Under 30 kGy Irradiation							
Cr-0.0	440	0.52	2.623	2.464	2.561	2.549	5.1879 X 10^{26}
Cr-0.2	455	0.5	2.945	2.810	2.905	2.886	4.5008 X 10^{32}
Cr-0.4	457	0.538	1.957	1.902	1.951	1.937	4.8809 X 10^{29}
Cr-0.6	458	0.535	1.456	1.324	1.420	1.400	7.1121 X 10^{21}
Cr-0.8	461	0.576	0.821	0.505	0.721	0.682	1.1172 X 10^{20}
Cr-1.0	459	0.6	1.181	1.014	1.130	1.109	8.906 X 10^{32}

The order of trap centers, and the outer most orbital (3d) degeneracy of Cr^{3+} ions lead to few order of covalence, which also results in good order of thermoluminescence with in the samples. The octahedral CrO_6 units act as modifiers induce non bridging oxygens, could lead to enhanced TL emission. The increase in Cr_2O_3 mol % from 0 to 0.8 mol % improves octahedral tendency of samples, which lead to variation in intensities of thermoluminescence glow curves. Thereafter TL results follows reverse trend. The existence of Ca^{2+} ions with in the samples also another the reason to for better thermoluminescence results of samples. The developed octahedral behavior added advantage to high order of TL emission.[23-24] The larger atomic radius of Cr^{3+} ions, tri-valent coordination of Cr^{3+} ions, octahedral tendency of Cr^{3+} ions, maximum intermolecular force between the ions, and short range periodic order with in the glasses are the reasons for the enhanced properties of the present glasses.

CONCLUSION

In the present work, we have synthesized the $Cr_xCa_{(10-x)}Al_{30}Si_{60}$ glasses, (where, 0.0 ≤ x≤ 1.0, step size = 0.2 mol %). The structure of the glasses studied by means of X-ray diffraction, DTA and FT-IR characterization. Under DTA Studies, evaluated thermal stabilities of glasses observed to be highest for Cr-0.8 glass code, which reveal, high order of octahedral Cr^{3+} ions. The electrical conductivity and thermoluminescence studies of glasses also reported; Observed, dc conductivity (~1.657 x10^{-4} ohm^{-1} cm^{-1}), and A.E. (~0.3669 eV) evaluations of glass with 0.8 mol% Cr_2O_3 concentration is a beneficial glass in electronics. The TL results such as shape symmetry factor and low AE's of Cr-0.8 glass code under thermoluminescence studies is a useful TL asset. The larger atomic radius of Cr^{3+} ions, tri-valent coordination of aluminum ions, octahedral tendency of Cr^{3+} ions, maximum intermolecular force between the ions, and short range periodic order with in Cr-0.8 glass code is the reason for the enhanced properties. Based on structure, electrical and thermoluminescent studies of the glasses recommend that the Cr-0.8 glass code is a desirable resource for electrical and thermoluminescent use.

ACKNOWLEDGMENT

The authors thank Management of Methodist College of Engineering and Technology, ABIDS, Telangana, INDIA for continuous moral support during the overall task.

REFERENCE

1. Jia-Jun He, Shao-Yi Wu, Li-Juan Zhang, Yong-Qiang Xu, and Chang-Chun Ding, *Journal of Non-Crystalline Solids*, **437**, 58(2016), https://doi.org/10.1016/j.jnoncrysol.2016.01.019

2. N Rama Krishna Chand, B K Sudhakar, G Ravi kumar, G Srinivasa Rao, and Ch Srinivasa Rao, *Physica Scripta,* **96(12)**, 125020(2021), https://doi.org/10.1088/1402-4896/abd202
3. M.S. Gaafar, S.Y. Marzouk, and I.S. Mahmoud, *Results in Physics*, **22**, 103944(2021), https://doi.org/10.1016/j.rinp.2021.103944
4. Padala Ashok, Ravi Kumar Guntu, and G. Bhikshamaiah, *Optik*, **206**, 164367(2020), https://doi.org/10.1016/j.ijleo.2020.164367
5. Byeongwon Park, Hong Li, and L.René Corrales, *Journal of Non-Crystalline Solids,* **297**, 220(2002), https://doi.org/10.1016/S0022-3093(01)00935-8.
6. Hirokazu Masai, Go Okada, Noriaki Kawaguchi, and, Takayuki Yanagida, *Journal of Non-Crystalline Solids*, **501**, 131(2018) https://doi.org/10.1016/j.jnoncrysol.2017.11.026
7. Padala Ashok, Ravi Kumar Guntu, G. Bhikshamaiah, Y. Markandeya, M. Madhu, Kore Anusha, N. Jahangeer, G. Anil Kumar, N. Ch. Sriman Narayana Iyengar, and Ch. Srinivasa Rao, *Journal of Luminescence*, **227**, 117473(2020), https://doi.org/10.1016/j.jlumin.2020.117473.
8. P. Goharian, B. Eftekhari Yekta, A.R. Aghaei, and S. Banijamali, *Journal of Non-Crystalline Solids*, **409**, 120(2015), https://doi.org/10.1016/j.jnoncrysol.2014.11.016.
9. G. Ravi Kumar, and M.C. Rao, *Optik,* **181**, 721(2019), https://doi.org/10.1016/j.ijleo.2018.12.110
10. Taoyong Liu, Cui Li, Qianxing Huang, Chenxing Liu, Changwei Lin, Qian Zhang, Zhiwei Luo, Ligang Zhu, and Anxian Lu, *Journal of Non-Crystalline Solids,* **543**, 120154(2020), https://doi.org/10.1016/j.jnoncrysol.2020.120154.
11. Ch. Rani, *Rasayan Journal of Chemistry,* **13**, 887(2020), http://dx.doi.org/10.31788/RJC.2020.1325582
12. M.C. Rao, and G. Ravi Kumar, *Optik,* **179**, 1109(2019), https://doi.org/10.1016/j.ijleo.2018.10.163
13. B. Mirhadi, and B. Mehdikhani, *Journal of Non-Crystalline Solids*, **357**, 3711(2011), https://doi.org/10.1021/jp111458f
14. R. K. Guntu, *Bulletin Material Science*, **42**, 214(2019), https://doi.org/10.1007/s12034-019-1892-3
15. K. V.. Rao, M. Madhu, P. Ashok, G. Anil Kumar, and R. K. Gutu, *Silicon*, **09**, 02 (2022), https://link.springer.com/article/10.1007/s12633-022-01731-6
16. G. R. Kumar, P. V. Reddy, M.C. Rao, Srikumar, and Ch. Srinivasa Rao, *Materials Research Express,* **05**, 035203(2018), https://doi.org/10.1088/2053-1591/aab4e6
17. F. S. De Vicente, F. A. Santos, B. S. Simões, S. T. Dias, M. Siu Li, *Optical Materials*, **38**, 119 (2014), http://dx.doi.org/10.1016/j.optmat.2014.10.012
18. G. Ravi Kumar, T. Srikumar, M.C. Rao, P. Venkat Reddy, and Ch. Srinivasa Rao, *Optik,* **161**, 250(2018), https://doi.org/10.1016/j.ijleo.2018.02.039.
19. G. Anil Kumar, Y. Rambabu, Ravi Kumar Guntu, K. Sivaram, M. Sreenath Reddy, Ch. Srinivasa Rao, V. Venkatramu, V. Ravi Kumar, and N. Ch. Sriman Narayana Iyengar, *Journal of the Mechanical Behavior of Biomedical Materials,* **119**, 104517(2021), https://doi.org/10.1016/j.jmbbm.2021.104517.
20. M. I. Sayyed, H. O. Tekin, and O. Agar, *Radiation Physics and Chemistry,* **163**, 58(2019), https://doi.org/10.1016/j.radphyschem.2019.05.012
21. R. K. Guntu, *Materials Science and Engineering: B,* **262,** 114784(2020), http://dx.doi.org/10.1016/j.mseb.2020.114784
22. R. Laopaiboon, and C. Bootjomchai, *Materials, and Design,* **80**, 20 (2015), https://doi.org/10.1016/j.matdes.2015.05.002
23. R. K. Guntu, *Journal of Molecular Structure*, **1248**, 131533(2021), https://doi.org/10.1016/j.molstruc.2021.131533
24. Nilo F. Cano, T.K. Gundu Rao, Jorge S. Ayala-Arenas, Carlos D. Gonzales-Lorenzo, Letícia M. Oliveira, and Shigueo Watanabe, *Journal of Luminescence*, **205**, 324(2019), https://doi.org/10.1016/j.jlumin.2018.09.034.

[RJC-6827/2021]